PINCH EFFECT IN A DEGENERATE PLASMA IN LONGITUDINAL AND TRANSVERSE MAGNETIC FIELDS

A. P. SHOTOV, S. P. GRISHECHKINA, and R. A. MUMINOV

P. N. Lebedev Physics Institute, Academy of Sciences, U.S.S.R.

Submitted to JETP editor August 5, 1966

J. Exptl. Theoret. Phys. (U.S.S.R.) 52, 71—78 (January, 1967)

We investigate the pinch effect of a degenerate electron-hole plasma of indium antimonide in the presence of longitudinal and magnetic electric fields. The plasma was produced by carrier injection resulting from passage of short ($\sim 10^{-6}$ sec) current pulses through rectifying contacts. The spectra and the intensity of the recombination radiation, and the electric conductivity of the plasma, were measured at 4.2°K. The longitudinal magnetic field was found to increase the radius of the plasma pinch in the quasi-stationary mode. A transverse magnetic field shifts the plasma pinch towards the surface of the crystal, and at large values of the field it causes heating of the carriers and destruction of the pinch. Estimates are presented for the main parameters of the plasma: the radius of the pinch, the concentration, the drift velocity, and the carrier mobility.

1. INTRODUCTION

WE have previously observed [1] magnetic compression (pinch effect) of a degenerate indium-antimonide plasma produced by carrier injection through contacts. Two methods were used for the investigation: 1) plasma spectroscopy using recombination radiation of the electron-hole pairs, 2) measurement of the electric conductivity of the plasma. In the present investigation we use these methods, supplemented by measurement of the intensity of the recombination radiation, to investigate the behavior of a plasma pinch in longitudinal and transverse magnetic fields.

The condition for the equilibrium of a cylindrical plasma pinch in a longitudinal magnetic field is the equality of the gaskinetic pressure of the plasma to the pressure of the magnetic field, which is the sum of the magnetic field of the current and the applied magnetic field. In integral form, this condition can be written as [2]

$$\bar{p} + \frac{\overline{H_i^2}}{8\pi} = \frac{H_\varphi^2(r_1)}{8\pi} + \frac{H^2(r_1)}{8\pi}, \qquad (1)$$

where $H_\varphi = 2J/cr_1$ is the magnetic field on the boundary of a pinch of radius r_1, $H(r_1)$ is the longitudinal magnetic field on the boundary of the pinch, and $\overline{H_i^2}$ is the square of the magnetic field intensity inside the plasma, averaged over the cross section area of the cylinder. In the case of a degenerate plasma, as is well known, the gaskinetic pressure is equal to

$$p = {}^2/_5 n\varepsilon_F. \qquad (2)$$

For a nondegenerate plasma $p = nkT$. Here n, ϵ_F, and T are the density, Fermi energy, and temperature of the carriers. It is seen from condition (1) that the magnetic field inside the pinch is added to the plasma pressure. Therefore a longitudinal magnetic field will spread the plasma if the field inside the plasma is larger than on the pinch boundary, and will compress the plasma in the opposite case. Whether the magnetic field will be attracted by the plasma pinch depends on the experimental conditions. This will be discussed later. The action of the transverse magnetic field on the plasma pinch turns out to be more complicated than described by (1) and will be considered in connection with a discussion of the measurement results.

2. EXPERIMENTAL PROCEDURE

A. Production of Degenerate Plasma

In order for the plasma to be degenerate a high carrier density is necessary, corresponding to the condition $\epsilon_F/kT > 1$, where

$$\varepsilon_F = \frac{h^2}{2m}\left(\frac{3n}{8\pi}\right)^{2/3}. \qquad (3)$$

For indium antimonide, where the effective mass of the electrons is very small, $m_e \sim 10^{-2}\, m_0$ (m_0 is the mass of the free electron), the electron gas at 4.2°K is strongly degenerate even at a density $\sim 10^{14}$ cm^{-3}.

In our case the degenerate plasma was produced by injecting carriers in a pure indium-antimonide crystal with current flowing through rectifying contacts. To prevent heating of the crystal, the injection was in short (10^{-6} sec) rectangular pulses with repetition frequency ~100 Hz. To ensure high injection efficiency, the p^+n and n^+n contacts were made by fusing-in alloys of In + 1% Cd and In + 1% Te in the [100] plane of the crystal. When current flowed in the forward direction, a double-injection mode is realized, with holes being injected from the p^+n contact and electrons from the opposite n^+n contact, producing a neutral electron-hole plasma in the volume of the crystal as a whole. At small currents, of the order of several milliamperes, the current-voltage characteristic had the negative-resistance region characteristic of double injection [3]. The cross-section area of the crystal was small, 0.5 × 0.5 mm, therefore at currents of approximately 10 A the carrier density in the plasma reached ~ 10^{16} cm^{-3}. At helium temperatures this corresponds to a very high degree of degeneracy of the electron gas $\epsilon_F/kC > 10$. The hole gas, owing to the large effective mass of the holes, $m_p/m_n \gg 1$, turned out to be in this case practically nondegenerate. During the injection we confined ourselves to maximum currents up to 20 A, which at a crystal thickness up to 0.5 mm does not lead to an appreciable heating of the electron gas by the electric field. Direct experimental proof of the degeneracy of the electron gas is the fact that stimulated and coherent emission was realized by us in similar crystals at 10°K [3], and 4.2°K [4].

B. Experimental Techniques

The sample for the measurement was placed in the helium bath of a metallic optical cryostat, which was located between the poles of an electromagnet. The internal helium-cooled windows of the cryostat were made of sapphire, and the external ones of fluorite. The current pulses from a miniature transistorized pulse generator [5] was fed to the sample through two coaxial stainless-steel tubes, forming a waveguide. The current and voltage pulses were observed on the screen of a double-beam high-frequency oscilloscope (type S1-7). In the measurements, the currents and the voltages were read at instants 0.7—0.3 μsec following the start of the pulse, corresponding to establishment of a stationary state between the electron-hole plasma and the lattice. In measuring the spectra, the 5.2-μ recombination radiation of the sample was focused by an LiF lens on the slit of a type IKM-1 monochromator with diffraction grating, making it possible to obtain a resolution up to 10^{-4} eV. The emission was registered with a photoresistance cooled to 80°K, the signal from which was recorded by an automatic potentiometer after amplification and synchronous detection.

In measuring the integral intensity, the recombination radiation of the sample was focused directly on the radiation receiver, bypassing the monochromator.

C. Measurement of the Magnetic Compression of Plasma by Means of the Spectra and Integral Intensity of the Radiation

The magnetic compression or spreading of the plasma pinch leads to a change in the carrier density per unit volume of the plasma. In the spectrum of the emission produced by interband recombination of the electron-hole pairs this is manifest in a shift of the maximum of the radiation and by an increase in the width of the spectrum. In the case of a degenerate plasma, the Fermi energy (and consequently also the carrier density in accordance with Eq. (3)) can be determined, accurate to kT, from the maximum of the emission spectrum, $\epsilon_F = h\nu_{max} - \epsilon_g$, [1] where ϵ_g is the width of the forbidden band of the semiconductor. In determining $h\nu_{max}$ it is necessary to take into account in the emission spectrum the correction for absorption, and in the case of ϵ_g it is necessary to take into account its small increase as a result of the Coulomb interaction between the carriers [6], which is manifest in a shift of the long-wave edge of the emission spectrum. In pure indium antimonide ϵ_g = 234 MeV, so that the emission spectrum lies in the region near 5 μ.

If we assume that the total number of carriers is maintained constant[1)], then the carrier density per unit volume in the case of magnetic compression of the plasma should increase in such a way that

$$n = (a/r_1)^2 n_0, \qquad (4)$$

where n = p is the average concentration of the electrons and holes in a pinch of radius r_1, $n_0 = p_0$ is the concentration of the electrons and holes in a crystal with dimension (radius) a.

The intensity of the recombination radiation (the number of quanta emitted per unit time and

[1)]The total number of carriers can change if the radiative recombination, and also the dependence of the injection on the electric field, have a strong influence on the particle balance.

per unit volume) in the case of interband recombination is quadratically related to the carrier density

$$i = \gamma np, \tag{5}$$

where γ is the coefficient of radiative recombination, which is assumed to depend little on the carrier energy. In observing the radiation intensity, a distinction can be made between two cases:

a) The integral emission from the entire surface of the crystal or from a unit length of the pinch is observed. In this case, as follows from (4) and (5), the relative increase in the intensity following magnetic contraction amounts to

$$I / I_0 = n / n_0 = a^2 / r_1^2. \tag{6}$$

b) The emission from a unit surface of the plasma pinch is observed, say by focusing the input slit of the monochromator on a definite area of the glowing surface of the pinch. In this case the relative increase of the integral intensity under magnetic contraction turns out to be larger and amounts to

$$I / I_0 = (n / n_0)^2 = (a / r_1)^4. \tag{7}$$

Thus, magnetic contraction can be revealed by the increase in the integral intensity. It should be noted, however, that the foregoing relations do not take into account absorption in the crystal, or the radiation produced by those carriers which still can remain outside the pinch after magnetic contraction. Their number should be determined by the number of ionized impurities which are present even in relatively pure crystals.

3. RESULTS AND DISCUSSIONS

Figure 1 shows the measured emission spectra at different values of the longitudinal magnetic field $H_Z \parallel J$. The spectrum 1 pertains to a plasma contracted only by the magnetic field of a current of 12 A ($H_Z = 0$). The succeeding spectra show that with increasing external longitudinal magnetic field, the intensity of radiation and the width of the spectrum decrease, while the maximum of the spectrum shifts towards the lower energies. A similar behavior is observed for all measured currents in the interval 5—18 A.

The measured integral intensity of the radiation from the crystal, as a function of the longitudinal magnetic field H_Z at definite values of the current, is shown in Fig. 2. The emission intensity at $H_Z = 0$ is taken as unity for all the currents. With increasing magnetic field, as can be seen from the figure, the integral intensity decreases. The intensity ceases to decrease in the magnetic fields H_Z = 250—300 Oe. The magnitude of the external longitudinal magnetic field then turns out to be of the order of H_φ—the magnetic field of the current in the plasma, if we use for estimates a current ~ 10 A and a pinch radius $r_1 = 0.7 \times 10^{-2}$ cm [1].

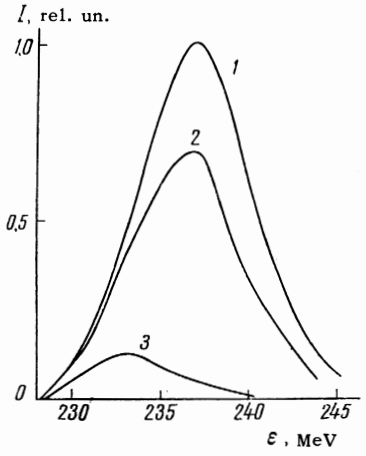

FIG. 1. Spectra of recombination radiation of a plasma at a current J = 12 A and T = 4.2°K for different values of the longitudinal magnetic field: 1 – $H_\parallel$ = 0, 2 – $H_\parallel$ = 50 Oe, 3 – $H_\parallel$ = 150 Oe; ϵ – radiation energy.

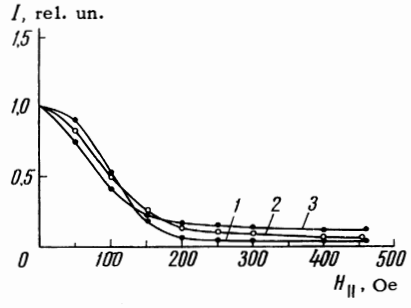

FIG. 2. Plasma radiation intensity of against a longitudinal magnetic field: 1 – J = 12 A, 2 – J = 9 A, 3 – J = 7 A.

The results of Figs. 1 and 2 can be attributed to spreading of the plasma pinch with increasing longitudinal magnetic field. This leads to a decrease in the carrier density per unit volume of the plasma pinch and consequently, in accord with (6) and (7), to a decrease in the integral intensity of the emission, to a decrease in the width of the emission spectra, and to a shift of the maximum of the spectrum towards lower energies. The fact that the intensity stops decreasing in magnetic fields H_Z = 250—300 Oe, means that the pinch has broadened so much that it reached the walls of the crystal, and the plasma fills the entire crystal. Therefore further increase in the magnetic field does not cause a decrease in the radiation intensity.

Broadening of a plasma pinch in a longitudinal

magnetic field was also observed in investigations of a nondegenerate plasma in a semiconductor [7-10] and in a hot plasma [11].

As noted in connection with Eq. (1) above, the spreading of the plasma in a longitudinal magnetic field will occur only if the field in the plasma pinch is stronger than outside the pinch. However, the possibility of such a capture of the magnetic field by the plasma is not obvious, since we are observing the pinch effect in a plasma of finite conductivity in a quasi-stationary state, where the condition $t \gg s$ is satisfied, where s is the time of magnetic diffusion:

$$s = a^2/4D = \pi\sigma a^2/c^2 \sim 10^{-10} \text{ sec.}$$

In the estimates we assumed that $n \sim 5 \times 10^{15}$ cm^{-3}, $\mu \sim 10^5$ cm^2/V-sec, and the plasma conductivity is $\sigma = en\mu \sim 10^{14}$ cgs esu.

In a poorly conducting plasma there should usually be no freezing-in of the magnetic force lines under such conditions. In our case, the magnetic field can become concentrated in the plasma because of the anisotropy of the conductivity along and across the magnetic field. In a helical magnetic field with components H_φ and H_z, the current will flow along helical lines, owing to the anisotropy of the conductivity. Therefore alongside with the current component J_z there appears an azimuthal component J_φ, which indeed produces the additional longitudinal field which combines with the initial field H_z [11]. The possibility of plasma paramagnetism of this type was considered theoretically by Braginskiĭ and Shafranov [2]. The conductivity anisotropy in a magnetic field can be appreciable in our case, since we deal with a plasma consisting of a degenerate electron gas and a nondegenerate hole gas, placed in a sufficiently strong magnetic field in which $\omega_c\tau \sim 1$ or, what is the same, $H\mu/c \sim 1$, where $H = 3 \times 10^2$ Oe, $\mu \sim 10^5$ cm^2/V-sec, ω_c is the cyclotron frequency, and τ is the mean free path time.

The difference in the conductivity along and across the magnetic field can be seen from the direct measurements of the electric conductivity of the plasma, the results of which are shown in Fig. 3. The plasma conductivity in a longitudinal magnetic field (curve 1) turns out to be much larger than in a transverse field (curves 3 and 4).

In connection with the data of Fig. 3, we can also note that the magnetoresistance makes it difficult to reveal magnetic contraction from the current-voltage characteristic. The radiation measurements fix the formation of the pinch with a current of 3 A at $H_z = 0$, whereas this is not

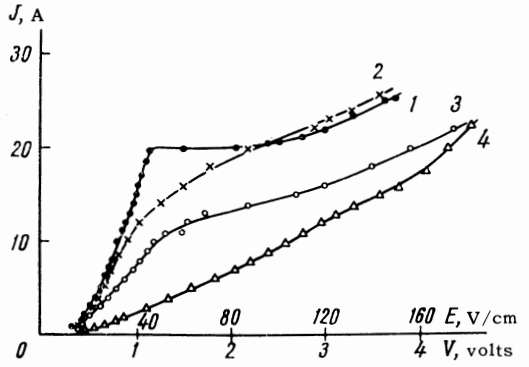

FIG. 3. Current vs. voltage of electron-hole plasma in longitudinal and transverse magnetic field: 1 – H = 0, 2 – $H_\parallel$ = 200 Oe, 3 – $H_\perp$ = 25 Oe, 4 – $H_\perp$ = 125 Oe.

very noticeable on the current-voltage characteristics. The sharp kink on the current-voltage characteristic, which sometimes appears in the pinch effect on Fig. 3 at J = 20 A, is apparently connected with instabilities that arise in the pinch.

The measured intensity of plasma emission from one of the faces of the crystal, in a transverse magnetic field, is shown in Fig. 4. In weak magnetic fields, up to ~ 50 Oe, the emission intensity increases, owing to the approach of the plasma pinch to the surface of the crystal, as was observed also by Osipov and Khvoshchev [10] in investigations of the pinch effect in a nondegenerate plasma. In our case, however, that of a relatively cold degenerate plasma in a transverse magnetic field, strong heating of the carriers is observed if

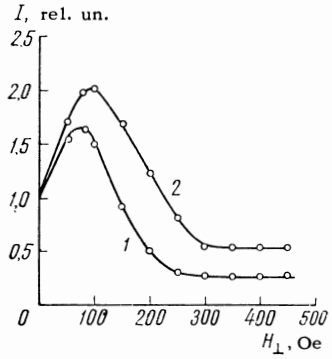

FIG. 4. Plasma radiation intensity vs. transverse magnetic field: 1 – J = 12 A, 2 – J = 9 A.

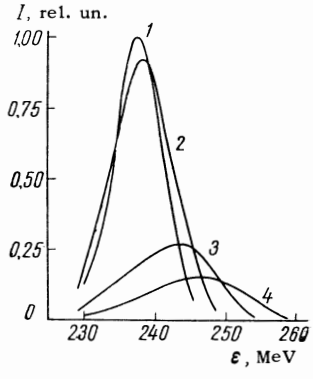

FIG. 5. Structures of recombination radiation of a plasma at a current J = 12 A and T = 4.2°K for different values of the transverse magnetic field: 1 – H = 0, 2 – $H_\perp$ = 50 Oe, 3 – $H_\perp$ = 100 Oe, 4 – $H_\perp$ = 150 Oe.

the current is maintained constant. This is revealed on the spectra of Fig. 5 by the shift of the maximum of the spectrum towards the higher energies and by the increase in the width of the spectrum. The carrier heating is already noticeable in magnetic fields of 50 Oe, and with further increase of the magnetic fields it leads to a lifting of the degeneracy. In the region of fields 100—300 Oe (at fixed current), a sharp decrease in intensity takes place, owing to the disintegration of the pinch by the increased gaskinetic pressure of the hot carriers (Figs. 4, 5). Simultaneously the current-voltage characteristic (Fig. 3) shows the existence of an increase in the plasma resistance in the transverse magnetic field.

In a relatively hot plasma [10], up to fields $H_\perp$ = 7 kOe, only the effect of motion of the pinch towards the surface of the crystal is observed; it is possible that in this case the carrier heating is not so noticeable compared with the rather high plasma temperature ($\sim 500°K$).

Using these results, and also the data of the carrier investigation [1], let us determine the main characteristics of the plasma. At the start of the magnetic contraction, when the plasma fills the entire crystal, the observed emission spectrum is distorted little by the absorption in the crystal. Therefore the Fermi energy can be determined from the emission spectrum most accurately. When H = 0, the pinch effect begins at J ~ 3 A; the corresponding Fermi energy is ϵ_F = 7 MeV. In the analysis of the emission spectra we took into account the decrease by approximately 3 MeV, of the width of the forbidden band with carrier density clearly revealed by the shift of the long-wave edge of the recombination-radiation spectrum. Using relation (3) and recognizing that $m_e = 2\times 10^{-2} m_0$, we obtain $n = 0.75\times 10^{16}$ cm^{-3}. The carrier drift velocity, determined by formula (7) from [1]:

$$J = \frac{4}{5}\frac{c^2}{e}\frac{\varepsilon_F}{v_z}, \qquad (8)$$

is found to be $v_z = 1.9\times 10^6$ cm/sec. On the current-voltage characteristic (Fig. 4) we have E = 21 V/cm at J = 3 A, and therefore the mobility is $\mu = 0.9\times 10^5$ cm^2/V-sec. At these values, in accordance with the relation

$$J/\pi r_1^2 = nev_z, \qquad (9)$$

the radius of the plasma pinch is r_1 = 0.20 mm, which is close to the dimension of the crystal a = 0.25 mm, as expected for the start of the magnetic contraction.

In the case of a longitudinal magnetic field, the condition (1) can be written in a form similar to (8):

$$\eta J = \frac{4}{5}\frac{c^2}{e}\frac{\varepsilon_F}{v_z}, \qquad (10)$$

where $\eta = 1 - (cr_1/2J)^2[\overline{H_i^2} - H^2(r_1)]$ is a coefficient characterizing the use of the magnetic field of the current for plasma contraction ($\eta = 1$ at $H_z = 0$). In currents larger than the critical value J = 3 A, the increase in the carrier density and in the width of the spectrum is due essentially to the magnetic contraction, whereas the number of injected carriers changes little. This is confirmed by the fact that, for example at J = 12 A and H_z = 150 Oe (Fig. 2), under conditions when the plasma fills almost the entire crystal, the position of the maximum of the spectrum is close to its position at 3 A. If we assume therefore that when J = 12 A and H_z = 200 Oe we have $n \approx 10^{16}$ cm^{-3} and $v_z = 2\times 10^6$ cm/sec, then, using (10), we obtain η = 0.3. This means that in a longitudinal magnetic field the pressure produced by the magnetic field of the current is essentially balanced by the counterpressure of the longitudinal field, and only a small part of the current pressure is offset by the plasma pressure.

At large currents, when the plasma contracts to a thin pinch, the electrodes, the distance between which is close to the transverse dimension of the crystal, can produce a noticeable deviation from the cylindrical-pinch geometry. For the same reason, and also because of the absorption of the radiation in the crystal, the use of the measurements of the spectra and of the intensity to calculate the pinch radius calls for certain caution in the case of strong contraction of the plasma. If we estimate the pinch radius by using the intensity data on Fig. 2, assuming at the same time that the number of carriers remains constant as the pinch broadens, then by using (6) we find that the pinch radius is $r_1 \approx 5\times 10^{-3}$ cm when J = 12 A and H_z = 0.

In semiconductor quantum generators, the magnetic contraction of the plasma, which leads to an increase in carrier density, can be used to produce population inversion. In ordinary quantum-generator constructions, however, where the coherent emission propagates in a direction perpendicular to the current, the pinch effect is an undesirable phenomenon, since the localization of the pinch inside the crystal leads to absorption of the radiation in the remaining part of the crystal.

In the plasma quantum generators developed by us [3,4] we used, to eliminate this phenomenon,

longitudinal magnetic fields which leads to an increase in the pinch radius. As shown by the foregoing data, magnetic fields of approximately 400 Oe are sufficient to broaden the pinch to the dimensions of the entire crystal (5×10^{-2} cm), if the current through the plasma is ~ 10 A. To attain the generation mode it becomes necessary sometimes to use large (quantizing) magnetic fields, which lead to an increase in the density of the states (at the Landau levels), so as to compensate for their radiation losses [3,4].

The transverse magnetic field can only bring the pinch closer to one of the crystal surfaces, but at the same time, as follows from the present results, this field causes strong heating of the carriers, and this hinders the possibility of producing population inversion.

The authors are grateful to B. M. Vul for interest in the work and remarks, and to A. V. Babushkin for help with the work.

[1] A. P. Shotov, S. P. Grishechkina, and R. A. Muminov, JETP 50, 1525 (1966), Soviet Phys. JETP 23, 1017 (1966).

[2] S. I. Braginskiĭ, and V. D. Shafranov, Fizika plazmy i problema upravleniya termoyadernykh reaktsiĭ (Plasma Physics and the Problem of Control of Thermonuclear Reactions), 2, AN SSSR, 1958, p. 26.

[3] A. P. Shotov, S. P. Grishechkina, B. D. Kopylovskiĭ, and R. A. Muminov, FTT 8, 1083 (1966), Soviet Phys. Solid State 8, 865 (1966).

[4] A. P. Shotov, S. P. Grishechkina, and R. A. Muminov, FTT 8, 2496 (1966), Soviet Phys. Solid State 8, 1998 (1967).

[5] B. D. Kopylovskii and V. S. Ivanov, PTÉ No. 4, 145 (1965).

[6] V. L. Bonch-Bruevich, FTT, coll. 2, 177 (1959).

[7] M. Glicksman and M. C. Steel, Phys. Rev. Lett. 2, 461 (1959).

[8] A. G. Chunoweth and A. A. Murray, Phys. Rev. 123, 515 (1961).

[9] B. Ancker-Johnson, R. Cohen, and M. Glicksman, Phys. Rev. 124, 1745 (1961).

[10] B. D. Osipov and A. N. Khvoshchev, JETP 43, 1179 (1962), Soviet Phys. JETP 16, 847 (1963).

[11] L. N. Artsimovich, Upravlyaemye termoyadernye reaktsii (Controlled Thermonuclear Reactions), Fizmatgiz, 1961, Sec. 6.4.

Translated by J. G. Adashko
9